Physics Letters B 692 (2010) 323–326

Contents lists available at ScienceDirect

Physics Letters B

www.elsevier.com/locate/physletb

Composite inelastic dark matter

Daniele S.M. Alves [a,b,*], Siavosh R. Behbahani [a,b], Philip Schuster [a], Jay G. Wacker [a]

[a] SLAC, Stanford University, Menlo Park, CA 94025, United States
[b] Physics Department, Stanford University, Stanford, CA 94305, United States

ARTICLE INFO

Article history:
Received 6 May 2010
Received in revised form 26 July 2010
Accepted 29 July 2010
Available online 5 August 2010
Editor: M. Cvetič

Keywords:
Inelastic dark matter
DAMA
Dark sector

ABSTRACT

Peaking consistently in June for nearly eleven years, the annual modulation signal reported by DAMA/NaI and DAMA/LIBRA offers strong evidence for the identity of dark matter. DAMA's signal strongly suggest that dark matter inelastically scatters into an excited state split by $\mathcal{O}(100\ \text{keV})$. We propose that DAMA is observing hyperfine transitions of a composite dark matter particle. As an example, we consider a meson of a QCD-like sector, built out of constituent fermions whose spin–spin interactions break the degeneracy of the ground state. An axially coupled $U(1)$ gauge boson that mixes kinetically with hypercharge induces inelastic hyperfine transitions of the meson dark matter that can explain the DAMA signal.

Published by Elsevier B.V. Open access under CC BY license.

This Letter proposes a new class of inelastic dark matter (iDM) models that can explain the annual modulation reported by DAMA/NaI and DAMA/LIBRA [1]. DAMA's signal peaks in early June, consistent with dark matter scattering, and has remained in phase for nearly eleven years. Moreover, the fractional modulation of the signal appears anomalously large, and the nuclear recoil spectrum has a peak near $E_R \simeq \mathcal{O}(30\ \text{keV})$.

The hypothesis that dark matter scatters inelastically off nuclei into a $\mathcal{O}(100\ \text{keV})$ excited state elegantly explains the salient features of the DAMA signal [2]. iDM models predict nuclear recoil spectra with a characteristic peak and an $\mathcal{O}(1)$ modulation fraction [3]. The large dark matter velocity threshold required by inelastic kinematics also implies that heavier nuclei targets like ^{127}I in DAMA provide enhanced signal sensitivity relative to lighter

and similar papers at core.ac.uk
brought to you by CORE
provided by Elsevier - Publisher Connector

posite dark matter particle. (For other examples of composite dark matter, see [4].) We illustrate this mechanism with a simple model where the majority of dark matter is a meson of a strongly coupled $SU(N_c)$ gauge sector that confines near $\Lambda \simeq$ GeV. These mesons are comprised of constituent fermions whose hyperfine interactions split the ground state by $\mathcal{O}(100\ \text{keV})$. When one constituent quark is non-relativistic, a hierarchy between the hyperfine scale and the dark matter mass follows inevitably from an enhanced spin symmetry. The dark matter couples to a new $U(1)_{A'}$ vector boson that kinetically mixes with the Standard Model's hypercharge [5]. Another version of iDM with kinetic mixing is given in [6]. Axial couplings of the $U(1)_{A'}$ to the constituent fermions mediate inelastic hyperfine transitions that dominate low-energy nuclear scattering.

The model considered here has two Dirac fermions, Ψ_H and Ψ_L, transforming in the fundamental representation of the $SU(N_c)$ gauge group. The new $U(1)_{A'}$ couples axially to $\Psi_{H,L}$, each of which have equal and opposite unit charge. We introduce a charge-2 Higgs ϕ, whose vacuum expectation value generates a mass for $\Psi_{H,L}$ and the A'. The $U(1)_{A'}$ is non-anomalous for this particle content. The dark matter candidate is a $\bar{\Psi}_L\Psi_H$ bound state, and its stability can be guaranteed by imposing a $U(1)_{H-L}$ flavor angian for this

$$\mathcal{L} = \mathcal{L}_{\text{SM}} + \mathcal{L}_{\Psi} + \mathcal{L}_{\text{Gauge}} + \mathcal{L}_{\text{break}}, \tag{1}$$

$$\mathcal{L}_{\text{Dark Gauge}} = -\frac{1}{2}\,\text{Tr}\,G_{\mu\nu}^2 - \frac{1}{4}F_{A'}^2 + \epsilon F_{A'}^{\mu\nu}B_{\mu\nu}; \tag{2}$$

$$\mathcal{L}_{\Psi} = \bar{\Psi}_L i\not{D}\Psi_L + y_L\bar{\Psi}_L\big(\phi\mathcal{P}_L + \phi^*\mathcal{P}_R\big)\Psi_L + \bar{\Psi}_H i\not{D}\Psi_H + y_H\bar{\Psi}_H\big(\phi^*\mathcal{P}_L + \phi\mathcal{P}_R\big)\Psi_H,$$

$$\mathcal{L}_{\text{break}} = |D_\mu\phi|^2 - \lambda\big(|\phi|^2 - v_\phi^2\big)^2,$$

where $\mathcal{P}_{L,R}$ are the left and right Dirac projection operators, and $D_\mu\Psi_{L,H} = (\partial_\mu + ig_D G_\mu \pm ie'\gamma_5 A'_\mu)\Psi_{L,H}$ where G_μ is the $SU(N_c)$ gauge field and $\pm$ corresponding to Ψ_H and Ψ_L, respectively. $B^{\mu\nu}$ is the hypercharge field strength, $F_{A'}^{\mu\nu}$ is the $U(1)_{A'}$ field strength, and $G_{\mu\nu}$ is the field strength for the confining $SU(N_c)$

* Corresponding author at: Physics Department, Stanford University, Stanford, CA 94305, United States.
E-mail address: alves@stanford.edu (D.S.M. Alves).

0370-2693 Published by Elsevier B.V. Open access under CC BY license.
doi:10.1016/j.physletb.2010.08.006

theory. In this model, the dark quarks have a hierarchy of masses $m_L = y_L v_\phi \leqslant \Lambda \ll m_H = y_H v_\phi$, and an A' mass in the range 100 MeV $\lesssim m_{A'} \lesssim$ 20 GeV.

At momenta beneath Λ, the model consists of mesons and baryons built out of Ψ_H and Ψ_L, listed below. Because $m_H \gg m_L$, we classify the states by the number of Ψ_H constituents, N_H. N_H Ψ_H can form bound states by anti-symmetrizing their color indices. They have binding energies

$$E_B \propto \alpha_t^2(\mu^*) m_H / N_c^2 \tag{3}$$

where $\alpha_t(\mu^*)$ is the running 't Hooft coupling of the strong gauge sector evaluated at the inverse Bohr radius of the bound state, $\mu^* \simeq \alpha_t m_H$. At distances greater than Λ^{-1}, the color charge of N_H heavy Ψ_H's can be screened by N_H light $\bar{\Psi}_L$ antiquarks to form a dark N_H-meson, or by $N_c - N_H$ Ψ_L quarks to form a dark N_H-baryon. The Ψ_H and Ψ_L quarks have antisymmetrized colors, so the spins of same-flavor constituents must be symmetrized. The resulting range of spins for dark mesons and baryons is

$$0 \leqslant j_{N_H \mathrm{M}} \leqslant N_H, \quad \left|\frac{1}{2}N_c - N_H\right| \leqslant j_{N_H \mathrm{B}} \leqslant \frac{1}{2}N_c. \tag{4}$$

Due to the spin–spin interactions, the lowest-spin configurations with a given N_H are the lowest-energy configurations. In particular, all dark mesons have a spin-0 ground state.

Cosmology dominantly produces $N_H = 1$, $J^P = 0^-$ mesons $\pi_\mathrm{d} = \bar{\Psi}_L \gamma_5 \Psi_H$, as will be shown later. In the limit $m_L \leqslant \Lambda \ll m_H$, the $J^P = 1^-$ vector $\rho_\mathrm{d} = \bar{\Psi}_L \gamma_\mu \Psi_H$ is nearly degenerate with π_d, and is accessible in low-energy π_d scattering. Spin–spin interactions generate a mass splitting

$$\Delta \equiv M_{\rho_\mathrm{d}} - M_{\pi_\mathrm{d}} = \frac{\kappa \Lambda^2}{M_{\pi_\mathrm{d}}}, \tag{5}$$

where $M_{\pi_\mathrm{d}} \simeq m_H$ is the π_d mass, and κ is an order-unity coefficient that fixes the relation between Δ and Λ. The π_d and ρ_d mesons form a multiplet of the $SU(2)_{H\text{-spin}}$ that rotates Ψ_H's spin. In the limit $m_H \gg \Lambda$, $SU(2)_{H\text{-spin}}$ is an approximate symmetry, guaranteed by Lorentz invariance. This is a familiar phenomenon in heavy-quark physics and the enhanced symmetry constrains low energy interactions of π_d and ρ_d mesons [7].

1. CiDM scattering

The low-energy scattering of the dark mesons arises after diagonalizing the kinetic mixing terms in (2), and integrating out the weak interactions. The dark matter constituents couple to the Standard Model via

$$\mathcal{L}_\mathrm{Int} = \frac{-\epsilon s_\theta}{m_{Z^0}^2} J_{Z^0 \mu} J_\mathrm{d}^\mu + \left(J_\mathrm{d}^\mu - \epsilon c_\theta J_\mathrm{EM}^\mu - \epsilon s_\theta \frac{m_{A'}^2}{m_{Z^0}^2} J_{Z^0}^\mu \right) A'_\mu, \tag{6}$$

where $s_\theta = \sin\theta_\mathrm{w}$ and $c_\theta = \cos\theta_\mathrm{w}$, J_EM is the electromagnetic current, J_{Z^0} is the neutral Z^0 current and J_d is the dark sector $U(1)_{A'}$ current,

$$J_\mathrm{d}^\mu = \bar{\Psi}_H \gamma^\mu \gamma_5 \Psi_H - \bar{\Psi}_L \gamma^\mu \gamma_5 \Psi_L. \tag{7}$$

As discussed in [8], parity-breaking by strong dynamics in the dark sector induces elastic charge-radius $\pi_\mathrm{d} + \mathrm{SM} \to \pi_\mathrm{d} + \mathrm{SM}$ scattering, which has new consequences for direct detection. For simplicity, we will discuss the case where the strong dynamics preserves parity in the dark sector, so that no $\pi_\mathrm{d} + \mathrm{SM} \to \pi_\mathrm{d} + \mathrm{SM}$ elastic scattering is mediated by the $U(1)_{A'}$ current in (7) to $\mathcal{O}(\epsilon)$. So long as ϕ does not significantly mix with the Standard Model Higgs boson, elastic dark-matter-nucleus scattering induced by ϕ exchange is also negligible.

Using heavy quark effective theory [7], the $SU(2)_{H\text{-spin}}$ and Lorentz symmetry of the π_d, ρ_d mesons constrain the form of their scattering matrix elements. At leading order in relative velocity, $v_\mathrm{rel}/c \simeq 10^{-3}$, the $\pi_\mathrm{d} \to \rho_\mathrm{d}$ matrix elements are given by

$$\left\langle \rho_\mathrm{d}(p', \epsilon) \middle| J_\mathrm{d}^\mu \middle| \pi_\mathrm{d}(p) \right\rangle \simeq 4 M_{\pi_\mathrm{d}} \epsilon_{p'}^\mu + \frac{c_\mathrm{in}}{\Lambda} (p + p')^\mu q_\nu \epsilon_{p'}^\nu, \tag{8}$$

where $\epsilon_{p'}^\mu$ is the polarization of ρ_d, and $c_\mathrm{in} \sim 1$ controls dipole scattering. We have dropped terms proportional to q^μ, which have vanishing contraction with the conserved Standard Model electromagnetic current. The second term in (8) leads to scattering enhanced by $q^2/v_\mathrm{rel}^2 \Lambda^2 \simeq 10^3$ relative to the first term.

In terms of relativistic effective operators, the low energy interactions can be described as:

$$\mathcal{L}_\mathrm{eff} = d_\mathrm{in} M_{\pi_\mathrm{d}} \pi_\mathrm{d}{}^\dagger \rho_\mathrm{d}{}^\mu A'_\mu + \frac{c_\mathrm{in}}{\Lambda} \pi_\mathrm{d}{}^\dagger \partial_\mu \rho_{\mathrm{d}\,\nu} F_{A'}^{\mu\nu} + \frac{d_\mathrm{el}}{\Lambda^2} \partial_\mu \pi_\mathrm{d}^\dagger \partial_\nu \pi_\mathrm{d} \tilde{F}_{A'}^{\mu\nu} + \cdots. \tag{9}$$

Elastic transitions mediated by the d_el-operator above are velocity suppressed relative to the inelastic ones. The axial coupling of A' to the fermionic constituents leads to a parity constraint on the interactions, forbidding elastic operators of the type

$$\mathcal{O}_\mathrm{forbidden} = \frac{c_\mathrm{el}}{\Lambda^2} \partial_\mu \pi_\mathrm{d}^\dagger \partial_\nu \pi_\mathrm{d} F_{A'}^{\mu\nu} \tag{10}$$

that if otherwise allowed would dominate over inelastic scattering.

Using (8), the low-energy inelastic cross-section for π_d to scatter off a nucleus of mass m_N and electric charge Z with nuclear recoil energy E_R is

$$\frac{d\sigma(E_R, v_\mathrm{rel})}{dE_R} \simeq \frac{4Z^2\alpha}{M_{\pi_\mathrm{d}} \Delta f_\mathrm{eff}^4} \frac{m_N^2 E_R |F_\mathrm{H}(E_R)|^2}{v_\mathrm{rel}^2 (1 + 2 m_N E_R / m_{A'}^2)^2}, \tag{11}$$

where

$$f_\mathrm{eff}^4 = m_{A'}^4 / (c_\mathrm{in} \epsilon c_\theta g_\mathrm{d})^2 \kappa \tag{12}$$

and F_H is the Helm nuclear form factor used in [10]. The differential scattering rate per unit detector mass is

$$\frac{dR}{dE_R} = \frac{\rho_0 v_0}{m_N M_{\pi_\mathrm{d}}} \int_{v_\mathrm{min}(E_R)} d^3 v_\mathrm{rel} \frac{v_\mathrm{rel}}{v_0} f(v; v_e) \frac{d\sigma}{dE_R}, \tag{13}$$

where $\rho_0 = 0.3$ GeV/cm^3 is the local density of dark matter, $v_\mathrm{min}(E_R)$ is the minimum relative velocity required to scatter with nuclear recoil energy E_R, and $f(v; v_e)$ is the dark matter velocity distribution function in the lab frame accounting for the Earth's variable velocity $\vec{v}_e$. Naively cutting off the velocity profile above the galactic escape velocity v_esc, we use the Standard Halo Model velocity distribution function,

$$f(v; v_e) \propto \left(e^{-(\vec{v} - \vec{v}_e)^2 / v_0^2} - e^{-v_\mathrm{esc}^2 / v_0^2} \right) \Theta\left(v_\mathrm{esc} - |\vec{v} - \vec{v}_e| \right). \tag{14}$$

Given the high uncertainty on the halo velocity distribution and the sensitivity of iDM models to it, we marginalize over the velocity parameters v_0 and v_esc, constrained to be in the range 150 km/s $\leqslant v_0 \leqslant$ 350 km/s and 480 km/s $\leqslant v_\mathrm{esc} \leqslant$ 650 km/s.

2. Direct detection

In DAMA, dark matter dominantly scatters off ^{127}I. The modulation spectrum and rate of the combined 1.17 ton-yr exposure [1] constrain the parameters in this model. We perform a global χ^2 fit by marginalizing over the 5 unknown parameters: M_{π_d}, Δ, f_eff, v_0 and v_esc.

Table 1
Summary of the data from null experiments.

Experiment	Element	Reference	Effective exposure	Period of run	Signal window	Obs. events
CDMS '05	Ge	[11]	34 kg-d	2005 Mar 25–2005 Aug 8	10–100 keV	1
CDMS '07	Ge	[12]	121.3 kg-d	2006 Oct 1–2007 Jul 1	10–100 keV	0
CDMS '08	Ge	[13]	194.1 kg-d	2007 Jul 1–2008 Sep 1	10–100 keV	2
XENON10	Xe	[14]	0.3×316.4 kg-d	2006 Oct 6–2007 Feb 14	4.5–75 keV	13
CRESST-II '04	W	[15]	$0.59 \times 0.9 \times 20.5$ kg-d	2004 Jan 31–2004 Mar 23	12–100 keV	5
CRESST-II '07	W	[16]	$0.59 \times 0.9 \times 48$ kg-d	2007 Mar 27–2007 Jul 23	12–100 keV	7
ZEPLIN-II	Xe	[17]	0.5×225 kg-d	2006 May 1–2006 Jun 30	13.9–55.6 keV	29
ZEPLIN-III	Xe	[18]	0.5×126.7 kg-d	2008 Feb 27–2008 May 20	10.7–30.2 keV	7
ZEPLIN-III (iDM)	Xe	[19]	0.5×63.3 kg-d	2008 Feb 27–2008 May 20	17.5–78.8 keV	5
XENON100	Xe	[20]	161 kg-d	2009 Oct 20–2009 Nov 12	7.4–29.1 keV	0

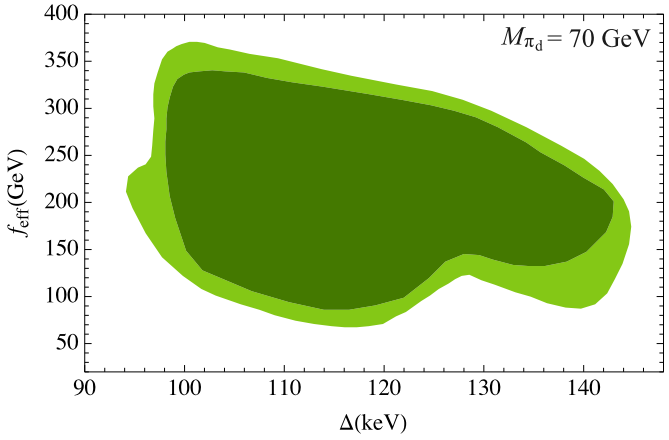

Fig. 1. Values of $f_{\rm eff}$, defined in (12), and Δ, defined in (5), that fit the DAMA/LIBRA signal and do not supersaturate the null searches at 2σ for a benchmark point of $M_{\pi_d} = 70$ GeV are shown in dark green (90% C.L.) and light green (99% C.L.).

Fig. 1 shows a benchmark mass of $M_{\pi_d} = 70$ GeV with 90 keV $\leqslant \Delta \leqslant 150$ keV and 50 GeV $\leqslant f_{\rm eff} \leqslant 400$ GeV. The 90% and 99% "confidence level" contours are plotted, corresponding respectively to $\chi^2 \leqslant \chi_0^2 + 9.3$ and $\chi^2 \leqslant \chi_0^2 + 15$, where χ_0^2 corresponds to the best fit point.

We compute the χ^2 using the 12 half-keVee bins of DAMA's modulated signal and reported error bars between 2 and 8 keVee, as well as the combined high energy bin from 8 to 12 keVee. This model fits DAMA's reported rate and nuclear recoil spectrum remarkably well. We also include in the χ^2 constraints from null searches summarized in Table 1, where for each null experiment we take as the standard error the 2σ Poisson fluctuation over the number of observed events. Moreover, we require the predictions for the null experiments not to supersaturate the observations at the (95% C.L.)

3. Cosmology

In the strongly coupled model of this Letter, Ψ_H and Ψ_L annihilate too efficiently for their thermal abundance to account for dark matter. Consequently, an asymmetry must be generated for "dark meson number," $n_M \propto n_H - n_L$. Dark mesogenesis could in principle be tied to the Standard Model's baryogenesis.

The π_d meson is a simple iDM candidate. Here we show that a dominant fraction of the dark meson number asymmetry resides in π_d mesons rather than exotic mesons, baryons, or ρ_d mesons.

Exotic mesons and baryons are seeded by Coulomb-like bound states of heavy quarks Ψ_H formed before confinement, or created by merging of π_d mesons after confinement.

Before confinement, the gluon entropy exponentially suppresses Ψ_H bound-state formation down to a temperature $T^* \simeq E_B/\ln(s/n_{\rm M}) \sim E_B/30$, where s is the entropy density of the Universe. For $N_c \geqslant 4$ and $M_{\pi_d} \lesssim \mathcal{O}(10^4)\Lambda$, $T^* \lesssim \Lambda$ so gluon entropy prevents Ψ_H bound-state formation with $N_H \geqslant 2$ until confinement.

At confinement, Ψ_L quark–antiquark pairs nucleate to screen the color charge of the Ψ_H. Confinement preferentially leads to the formation of $N_H = 1$ dark meson over higher-N_H dark mesons or baryons. High-N_H dark meson formation is negligible because the Ψ_H are dilute at the time of confinement. Formation of $N_H = 1$ dark baryons is Boltzmann-suppressed for $N_c \gtrsim 4$ because they have $(N_c - 2)$ more Ψ_L constituents than dark mesons, so they are heavier.

After confinement, heavy-quark binding occurs via $\pi_d + \pi_d \to \pi_d^{(2)} + G$, where G is a glueball and $\pi_d^{(2)}$ is an $N_H = 2$ dark meson. For $\Lambda \sim \mathcal{O}(1\text{ GeV})$ and $m_H \sim \mathcal{O}(100\text{ GeV})$, these reactions are *endothermic* because the glueballs have a mass $m_G = \mathcal{O}(\Lambda) \gtrsim E_B$. The binding reactions of Ψ_H require large momentum transfer $p_{\rm min} \sim \sqrt{m_{\pi_d}(m_G - E_B)} \gg \Lambda$, so the binding cross-section is controlled by perturbative Ψ_H dynamics. The thermally averaged π_d binding cross-section is parametrically

$$\langle \sigma v \rangle \sim e^{-(m_G - E_B)/T} \frac{\alpha_t^2(p_{\rm min})}{N_c^2 m_H^2}, \tag{15}$$

which is Boltzmann-suppressed for endothermic binding reactions.

To summarize, Ψ_H binding is suppressed by entropy for $T \leqslant \Lambda$, and by the endothermic Boltzmann factor for $T \geqslant \Lambda$. In fact, $N_H \neq 1$ dark mesons have spin-0 ground states and similar scattering properties to π_d, so their abundances can be significant. Constraints arise only from $N_H = N_c$ dark baryons, with potentially large elastic scattering cross-sections. Baryon formation proceeds through a sequence of Ψ_H-binding reactions, so a mild suppression of the binding rate at each stage significantly suppresses baryon formation. This is discussed in detail in [9].

The nearly degenerate $N_H = 1$ meson spin states π_d and ρ_d are equally populated at high temperatures. If the ρ_d decays only through kinetic mixing with hypercharge, the only kinematically allowed decays are to π_d plus photons or neutrinos. These decays have lifetime longer than the age of the Universe [21]. Constraints from direct detection of $\rho_d \to \pi_d$ de-excitation in nuclear scattering imply a fractional number-density bound $n_{\rho_d}/n_{\pi_d} \lesssim 10^{-2}$ [21]. This constraint is endemic to all iDM models coupled to the Standard Model only through kinetic mixing, and is troublesome if kinetic decoupling of dark matter occurs before $T \simeq 100$ keV. However, in CiDM models, ρ_d is de-excited through $\rho_d + \rho_d \to \pi_d + \pi_d$ scattering, with a large cross section set by the size of the dark meson, $\langle \sigma_{\rho_d\rho_d \to \pi_d\pi_d} v \rangle \simeq \Lambda^{-2}$. For $M_{\pi_d} \sim 100$ GeV and $\Lambda \sim 1$ GeV, this reaction freezes out when $\exp(-\Delta/T_{\rm spin}) \equiv n_{\rho_d}/n_{\pi_d} \lesssim 10^{-3}$, where $T_{\rm spin} \lesssim \Delta$ is the asymptotic spin temperature. After structure formation begins, up-scattering of π_d into ρ_d can occur in dark matter halos, but the π_d–π_d scattering is endothermic and

the rate too small to re-populate the $\rho_{\rm d}$ state to an observable level today.

Even though the CiDM self-scattering cross-section is large enough to depopulate the $\rho_{\rm d}$ abundance, it is nevertheless consistent with current bounds on dark-matter self-interactions (see Table I of [22])

$$\frac{\sigma}{m} \simeq 2 \times 10^{-6}\ \frac{\rm cm^2}{\rm g} \left(\frac{\rm GeV}{\Lambda}\right)^2 \left(\frac{100\ \rm GeV}{M_{\pi_{\rm d}}}\right).$$

That is safely beneath the strongest present limits of $\sigma/m \lesssim 10^{-2}\ \rm cm^2/g$.

4. Discussion

The CiDM framework implements iDM in a parametrically novel manner. There are many generalizations of the model proposed in this Letter – for example, baryons and weakly coupled bound states ("atoms") [23]. Many of these generalizations also naturally posses large cross sections to de-excite the $\mathcal{O}(100\ \rm keV)$ excited state in the early Universe [21]. In contrast to weakly interacting iDM models, strongly interacting CiDM naturally leads to low spin temperatures and avoids de-excitation constraints.

The recoil spectrum predicted by (11) differs from conventional iDM spectra by a factor $\propto E_R$, offering a potential means of discriminating CiDM from iDM through direct detection. Moreover, specific CiDM models predict the existence of dark matter sub-components that arise from the small fraction of $\pi_{\rm d}$ mesons that do process into other dark hadrons. Detection of these dark matter sub-components provides a striking signature of the underlying dynamics of CiDM [9].

The $U(1)_{A'}$ discussed in this Letter has purely axial vector couplings to the dark quarks. Other charge assignments give rise to qualitatively different direct detection signatures, such as admixtures of elastic and inelastic scatterings. Many of these alternate charge assignments generate elastic transitions of dark matter with distinctive nuclear recoil spectra in addition to the inelastic transition [24].

DAMA prefers $f_{\rm eff} \simeq 300$ GeV, resulting in $m_{A'} \lesssim 30$ GeV, well beneath the energy frontier. Searches at high-intensity e^+e^- machines for CiDM through A' production of light Ψ_L matter may confirm or refute this entire class of models [25]. The coming generation of collider searches and direct detection experiments will determine the true nature of DAMA's signal, possibly leading to irrefutable signatures of dark matter, and may unveil a whole new sector of physics.

Acknowledgements

We thank Rouven Essig and Natalia Toro for numerous illuminating discussions, and Mariangela Lisanti for collaboration in setting constraints. We also thank Savas Dimopoulos, Michael Peskin, and Neal Weiner for helpful feedback. S.R.B., P.C.S. and J.G.W. are supported by the US DOE under contract number DE-AC02-76SF00515. D.S.M.A. is supported by the NSF under grant PHY-0244728.

References

[1] R. Bernabei, et al., Int. J. Mod. Phys. D 13 (2004) 2127, arXiv:astro-ph/0501412; R. Bernabei, et al., DAMA Collaboration, Eur. Phys. J. C 56 (2008) 333, arXiv:0804.2741 [astro-ph]; R. Bernabei, P. Belli, F. Cappella, et al., arXiv:1002.1028 [astro-ph.GA].
[2] D. Tucker-Smith, N. Weiner, Phys. Rev. D 64 (2001) 043502, arXiv:hep-ph/0101138.
[3] S. Chang, G.D. Kribs, D. Tucker-Smith, N. Weiner, arXiv:0807.2250 [hep-ph]; S. Chang, A. Pierce, N. Weiner, arXiv:0808.0196 [hep-ph].
[4] S. Nussinov, Phys. Lett. B 165 (1985) 55; R.S. Chivukula, T.P. Walker, Nucl. Phys. B 329 (1990) 445; J. Bagnasco, M. Dine, S.D. Thomas, Phys. Lett. B 320 (1994) 99, arXiv:hep-ph/9310290; R. Foadi, M.T. Frandsen, F. Sannino, arXiv:0812.3406 [hep-ph]; S.B. Gudnason, C. Kouvaris, F. Sannino, Phys. Rev. D 74 (2006) 095008, arXiv:hep-ph/0608055; M.Y. Khlopov, arXiv:0806.3581 [astro-ph].
[5] B. Holdom, Phys. Lett. B 166 (1986) 196.
[6] N. Arkani-Hamed, D.P. Finkbeiner, T.R. Slatyer, N. Weiner, Phys. Rev. D 79 (2009) 015014, arXiv:0810.0713 [hep-ph].
[7] H. Georgi, Phys. Lett. B 240 (1990) 447.
[8] M. Lisanti, J.G. Wacker, arXiv:0911.4483 [hep-ph].
[9] D.S.M. Alves, S.R. Behbahani, P. Schuster, et al., JHEP 1006 (2010) 113, arXiv:1003.4729 [hep-ph].
[10] J.D. Lewin, P.F. Smith, Astropart. Phys. 6 (1996) 87.
[11] D.S. Akerib, et al., CDMS Collaboration, Phys. Rev. Lett. 96 (2006) 011302, astro-ph/0509259.
[12] Z. Ahmed, et al., CDMS Collaboration, arXiv:0802.3530 [astro-ph].
[13] Z. Ahmed, et al., CDMS-II Collaboration, Science, submitted for publication, arXiv:0912.3592 [astro-ph.CO].
[14] J. Angle, et al., XENON Collaboration, Phys. Rev. Lett. 100 (2008) 021303, arXiv:0706.0039 [astro-ph]; J. Angle, et al., XENON10 Collaboration, Phys. Rev. D 80 (2009) 115005, arXiv:0910.3698 [astro-ph.CO].
[15] G. Angloher, C. Bucci, P. Christ, et al., Astropart. Phys. 23 (2005) 325, astro-ph/0408006.
[16] G. Angloher, et al., arXiv:0809.1829 [astro-ph].
[17] G.J. Alner, H.M. Araujo, A. Bewick, et al., Astropart. Phys. 28 (2007) 287, astro-ph/0701858.
[18] V.N. Lebedenko, et al., arXiv:0812.1150 [astro-ph].
[19] D.Y. Akimov, H.M. Araujo, E.J. Barnes, et al., arXiv:1003.5626 [hep-ex].
[20] E. Aprile, et al., XENON100 Collaboration, arXiv:1005.0380 [astro-ph.CO].
[21] D.P. Finkbeiner, T. Slatyer, N. Weiner, I. Yavin, arXiv:0903.1037 [hep-ph]; B. Batell, M. Pospelov, A. Ritz, arXiv:0903.3396 [hep-ph].
[22] M.R. Buckley, P.J. Fox, Phys. Rev. D 81 (2010) 083522, arXiv:0911.3898 [hep-ph].
[23] D.E. Kaplan, G.Z. Krnjaic, K.R. Rehermann, et al., JCAP 1005 (2010) 021, arXiv:0909.0753 [hep-ph].
[24] M. Lisanti, J.G. Wacker, arXiv:0911.1997 [hep-ph].
[25] R. Essig, P. Schuster, N. Toro, arXiv:0903.3941 [hep-ph]; J.D. Bjorken, R. Essig, P. Schuster, N. Toro, arXiv:0906.0580 [hep-ph].